Optical coherence photoacoustic microscopy: accomplishing optical coherence tomography and photoacoustic microscopy with a single light source

Xiangyang Zhang
Hao F. Zhang
Shuliang Jiao

Optical coherence photoacoustic microscopy: accomplishing optical coherence tomography and photoacoustic microscopy with a single light source

Xiangyang Zhang,[a] **Hao F. Zhang,**[b] **and Shuliang Jiao**[a]
[a]University of Southern California, Keck School of Medicine, Department of Ophthalmology, Los Angeles, California 90033
[b]Northwestern University, Department of Biomedical Engineering, Evanston, Illinois 60208

Abstract. We developed optical coherence photoacoustic microscopy (OC-PAM) to demonstrate that the functions of optical coherence tomography (OCT) and photoacoustic microscopy (PAM) can be achieved simultaneously by using a single illuminating light source. We used a pulsed broadband laser centered at 580 nm and detected the absorbed photons through photoacoustic detection and the back-scattered photons with an interferometer. In OC-PAM, each laser pulse generates both one OCT A-line and one PAM A-line simultaneously; as a result, the two imaging modalities are intrinsically co-registered in the lateral directions. *In vivo* images of the mouse ear were acquired to demonstrate the capabilities of OC-PAM. © *2012 Society of Photo-Optical Instrumentation Engineers (SPIE).* [DOI: 10.1117/1.JBO.17.3.030502]

Optical coherence tomography (OCT)[1,2] and photoacoustic microscopy (PAM)[3–7] are two microscopic three-dimensional noninvasive imaging modalities that are based on different contrast mechanisms. OCT is a low-coherence interferometer-based optical imaging modality that provides imaging of mainly the scattering properties of biological tissues. By using a broadband light source, OCT resolves the depth of a scatterer through coherence gating. In contrast, PAM is an optical-absorption based imaging modality that detects laser-induced ultrasonic waves as a result of specific optical absorption.[8,9] When short laser pulses irradiate biological tissues, optical energy is absorbed by substances like hemoglobin and melanin, etc. and converted to heat. Thermo-elastic expansions then occur, which leads to generation of wideband ultrasonic waves. The ultrasonic waves are detected by an ultrasonic transducer to form an image.

Address all correspondence to: Shuliang Jiao, University of Southern California, Keck School of Medicine, Department of Ophthalmology, 1450 San Pablo St., Room DVRC 307E, Los Angeles, California 90033; E-mail: sjiao@usc.edu

Due to their different contrast mechanisms, OCT and PAM provide different yet complementary information of biological tissues. OCT images the microanatomy of a sample, e.g., the histology like cross-sectional image or the blood flow velocity by measuring the Doppler effect impinged on the probing light. In contrast, PAM maps the spatial distribution of light absorbers, e.g., hemoglobin, and is able to image the microvasculature and the associated blood oxygenation.[8]

Previously, the light sources used in OCT and PAM were different: OCT used broadband and continuous light, e.g., superluminescent diode (SLD), or virtually continuous light, e.g., Ti: Sapphire laser with ~80 MHz pulse repetition rate (PRR); PAM used narrow band and pulsed lasers. Another apparent difference in their light sources is that OCT used mainly near infrared (NIR) light for deeper penetration depth, while PAM usually uses visible light to target the absorption of hemoglobin. However, this apparent difference in wavelength does not forbid the use of visible light for OCT or NIR light for PAM. As an example, an OCT working in the visible spectrum[10] was built for imaging the spectral contrast of the retinal nerve fiber layer for glaucoma research, while NIR light has been used in PAM for imaging fatty tissues.[11] The selection of wavelength in PAM depends on the absorption spectrum of the targeted molecules.

The motivation for the reported technology development, optical coherence photoacoustic microscopy (OC-PAM), is that if we use a pulsed broadband laser we can simultaneously achieve both the PAM function and the OCT function from a single light source by detecting the corresponding photoacoustic and light signals. With this detection scheme each laser pulse will generate an A-scan for both OCT and PAM, respectively. Furthermore, this combination will generate registered PAM and OCT images, which offers a unique opportunity for studying the scattering and absorption of biological tissues.

Figure 1 shows a schematic of the experimental system. A custom built broadband dye laser pumped by a frequency-doubled Q-switched Nd:YAG (neodymium-doped yttrium aluminum garnet) laser (SPOT-10-100-532, Elforlight Ltd, UK: 532 nm; 10 μJ/pulse; 2 ns pulse duration; 30 kHz pulse repetition rate) was used as the illumination source. The output light has a center wavelength of 580 nm and a bandwidth of 20 nm [Fig. 2(a)]. The currently achievable PRR of the dye laser is 5 kHz. The output light was coupled into a single mode optical fiber (SMF). After exiting the SMF the light was collimated and directed into the source arm of a free-space Michelson interferometer. A beam-splitter cube split the input light into the sample and reference arms. In the reference arm, a BK7 glass plate was used to compensate for the group-velocity dispersion mismatch between the two interfering arms. In the meantime, the reflected light from the front surface of the glass plate was detected by a photodiode, the output signal of which was used to trigger the data acquisition of the ultrasonic signal. In the sample arm, the light was scanned by an *x-y* galvanometer scanner and was focused on the sample by an achromatic lens ($f = 19$ mm). The combined reflected light from the sample and reference arms was first coupled into a SMF and then detected by a spectrometer. The spectrometer consisted of a transmission grating (1800 lp/mm, Edmund), an imaging lens ($f = 150$ mm), and a line scan CCD camera (Aviiva-SM2-CL-2010, 2048 pixels operating in 12-bit mode, e2V). The sample clock of an analogue output
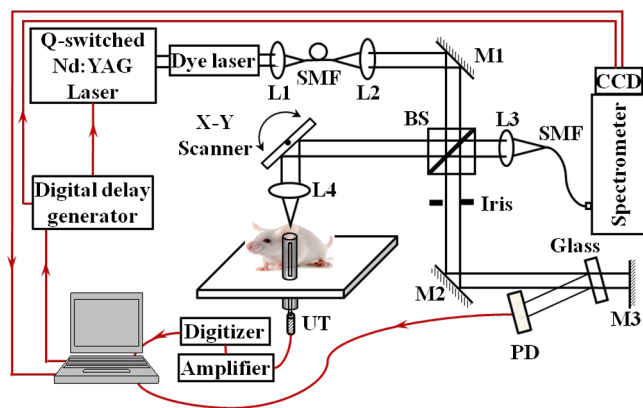
Fig. 1 Schematic of the experimental system of a free-space OC-PAM. L1 to L4: lens; BS: beam splitter; SMF: single mode fiber; PD: photodiode; UT: ultrasonic transducer; M1, M2: mirror.

board, which controlled the *x-y* galvanometer scanner, triggered a digital delay generator (DG645, Stanford Research Systems). Two outputs of the digital delay generator were used to trigger the CCD camera and laser, respectively.

The induced photoacoustic waves from the sample were detected by a custom-built needle ultrasonic transducer (30 MHz; bandwidth: 50%; active element diameter: 0.4 mm). The detected photoacoustic (PA) signals were first amplified by 80 dB and then digitized and stored by a high speed 14-bit digitizer (PCI-5122, National Instruments) at a sampling rate of 100 MS/s. The laser pulse energy was measured to be 200 nJ at the sample surface. As reported in our previous publications,[12–14] the depth resolution of the PAM imaging mode is 23 μm. During imaging, the ultrasonic transducer was inserted into a plastic tube filled with ultrasonic gel, which was placed under and in touch with the imaging subject. The distance between the ultrasonic transducer and the imaging subject was about 6 mm.

To test for biological imaging, we imaged the ears of a Swiss Webster mouse (Simonsen; body weight: 28 g) *in vivo*. After the hairs on one of the ears were gently removed with commercial nonirritating hair-removing lotion, the animal was placed on a homemade animal holder for imaging. Animals were anesthetized 5 minutes before the experiments by intraperitoneal (IP) injection of a cocktail containing Ketamine (54 mg/kg body weight) and Xylazine (6 mg/kg body weight). All experiments

were performed in compliance with the guidelines of the University of Southern California's Institutional Animal Care and Use Committee.

Figure 2 shows the measured spectrum of the light source and the corresponding point-spread-function (PSF) of the OCT mode. The spectrum was low-pass filtered to remove the spectral noise. The PSF was measured with a mirror as the sample and the path length difference was set at 0.5 mm. As shown in the figure, the measured depth resolution is 9.5 μm in air. During experiment, the exposure time of the CCD camera was set to 10 μs, which is about the shortest exposure time allowed by the CCD camera.

Figure 3 shows the simultaneously acquired OCT [Fig. 3(a)] and PAM [Fig. 3(b)] B-scan images of a mouse ear. Figure 3(c) shows the maximum-amplitude-projection (MAP) of the PA dataset. The 3D PAM data consist of 256 × 256 A-lines covering an area of 1.6 × 1.6 mm². The position of the B-scan images is marked on the MAP image as a dashed horizontal line. The vertical lines highlight the corresponding positions of the recognized blood vessels in the PAM B-scan image.

Although originated from the same photons, the OCT and PAM B-scan images show different features of the sample, which reflect their different imaging contrast mechanisms. In the OCT image, the depth resolution is sufficient to resolve different anatomical features including epidermis, dermis, and the cartilaginous backbone.[15] Due to the higher scattering coefficient of biological tissues in the visible spectrum, the achievable imaging depth of the OCT mode is reduced compared with an OCT in NIR. In our previous work on imaging, the mouse ear with an OCT in the 830 nm band[11] the whole thickness from the front to the back surfaces of the ear can be imaged. Here, we can see that the image can only reach about half of the thickness of the mouse ear. In the PAM image, the blood vessels appear as clusters of high amplitude ultrasonic signals while we do not have information about the anatomy of the tissue, where there is no significant absorption of the illuminating laser light.

Since both OCT and PAM images are generated from the same photons, they are automatically and precisely co-registered in the lateral directions, which are determined by the optical scanning. Figure 4 shows an example of fusing the OCT, and PAM images of Fig. 3, show that the blood vessels are pseudo-colored red in the PAM B-scan image.

Due to the high noise level of the spectrum of the laser pulses the quality of the OCT image acquired by the current system is not as good as those from the state-of-the-art SD-OCT images in
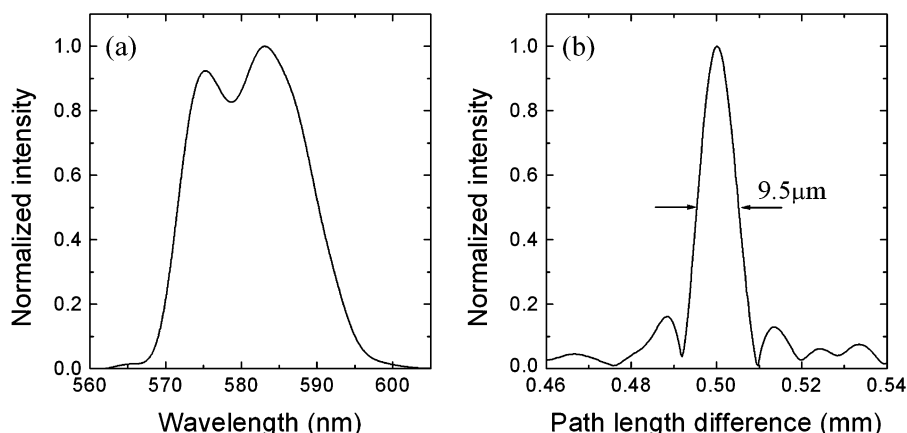

Fig. 2 Performance of the OCT mode. (a) The measured spectrum of the light source. (b) The calculated PSF of the OCT subsystem.
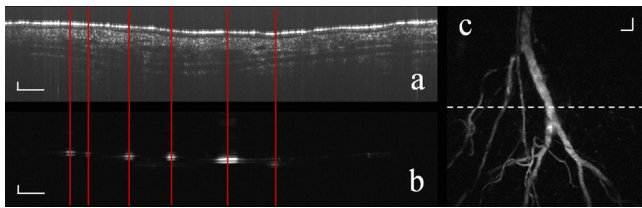
Fig. 3 OCT and PAM B-scan images acquired simultaneously *in vivo*. (a) OCT B-scan image; (b) PAM B-scan image, and (c) maximum-amplitude-projection (MAP) of the 3D PAM dataset. The vertical lines marked the corresponding locations of the recognized blood vessels. The horizontal line in the MAP image marks the location of the displayed B-scans; bar: 100 μm.
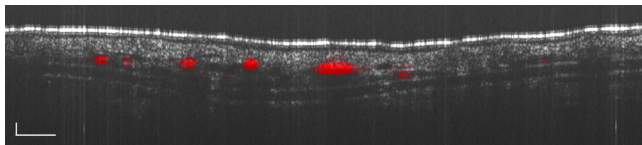

Fig. 4 Fused OCT and PAM images shown in Fig. 3; bar: 100 μm.

the 830 nm band,[11,16] which is the major weakness of the technology. The spectral noise can only be reduced by utilizing pulsed light source with stable spectral performance. We can foresee that by using a light source with stable spectral performance the image quality can be improved significantly.

The current laser light is in the visible spectrum targeting on the absorption of hemoglobin in the blood vessels. For targeting on other substance in the biological tissues, e.g., melanin, an OC-PAM can work in the NIR spectral range. When NIR light is used, the OCT mode will have better penetration and better imaging depth, while the absorption of hemoglobin will be weaker. We foresee that NIR OC-PAM will be suitable for imaging melanin in the retinal pigment epithelium (RPE). We recently have successfully demonstrated imaging the RPE with PAM working at a wavelength of 1 μm.[17]

One potential advantage of OC-PAM, which hasn't been demonstrated in our current experiments due to the noise level of the light source spectrum, is the short pulsed light for OCT. In conventional continuous wave-based SD-OCT system, any change of the sample, e.g., blood flow, during the exposure time of the camera (typically >10 μs) cannot be revealed. Since the pulse width of OC-PAM is in the ns level much faster transient process may be captured.

In conclusion, we have successfully demonstrated for the first time the feasibility of OC-PAM: generating OCT and PAM images with the same photons. By using a pulsed broadband laser as the illuminating light, OC-PAM can image the scattering and absorption contrasts simultaneously. It differs from the conventional concept of combining OCT and PAM by using different photons.[11] It is so named because OCT and PAM are an integral part of the technology. Currently, the image quality of the OC-PAM is limited mainly by the spectral noise of the laser pulse. Our current study is just a proof of concept. Future development will focus on

1. Improving the image quality by using a better pulsed broadband light source, e.g., a pulsed SLD.

2. Increasing the PRR of the light source to achieve higher imaging speed.

3. Shifting the laser spectrum to NIR for better imaging depth and ophthalmic applications.

4. Extracting quantitative information from the simultaneous multimodal images. Since the OC-PAM images are provided by the same photons, it may provide an unprecedented platform for the study of optical absorption and scattering in biological tissues.

Acknowledgments

References

1. D. Huang et al., "Optical coherence tomography," *Science* **254**(5035), 1178–1181 (1991).
2. M. Wojtkowski et al., "Ultrahigh-resolution, high-speed, Fourier domain optical coherence tomography and methods for dispersion compensation," *Opt. Express* **12**(11), 2404–2422 (2004).
3. K. Maslov et al., "Optical-resolution photoacoustic microscopy for *in vivo* imaging of single capillaries," *Opt. Lett.* **33**(9), 929–931 (2008).
4. H. Zhang et al., "Functional photoacoustic microscopy for high-resolution and noninvasive *in vivo* imaging," *Nat. Biotechnol.* **24**(7), 848–851 (2006).
5. H. Zhang, K. Maslov, and L. Wang, "*In vivo* imaging of subcutaneous structures using functional photoacoustic microscopy," *Nat. Protocols* **2**(4), 797–804 (2007).
6. H. Zhang et al., "Imaging acute thermal burns by photoacoustic microscopy," *J. Biomed. Opt.* **11**(5), 054033 (2006).
7. S. Hu and L. V. Wang, "Photoacoustic imaging and characterization of the microvasculature," *J. Biomed. Opt.* **15**(1), 011101–011115 (2010).
8. L. V. Wang, "Multiscale photoacoustic microscopy and computed tomography," *Nat. Photonics* **3**(9), 503–509 (2009).
9. Yi Wang, Chunhui Li, and Ruikang K. Wang, "Noncontact photoacoustic imaging achieved by using a low-coherence interferometer as the acoustic detector," *Opt. Lett.* **36**(20), 3975–3977 (2011).
10. X. Zhang et al., "Dual-band spectral-domain optical coherence tomography for *in vivo* imaging the spectral contrasts of the retinal nerve fiber layer," *Opt. Express* **19**(20), 19653–19659 (2011).
11. H. Wang et al., "Label-free bond-selective imaging by listening to vibrationally excited molecules," *Phys. Rev. Lett.* **106**(23), 238106 (2011).
12. S. Jiao et al., "Simultaneous multimodal imaging with integrated photoacoustic microscopy and optical coherence tomography," *Opt. Lett.* **34**(19), 2961–2963 (2009).
13. S. Jiao et al., "Photoacoustic ophthalmoscopy for *in vivo* retinal imaging," *Opt. Express* **18**(4), 3967–3972 (2010).
14. H. Zhang et al., "Collecting back-reflected photons in photoacoustic microscopy," *Opt. Express* **18**(2), 1278–1282 (2010).
15. Peter T. C. So, Hyun Kim, and Irene E. Kochevar, "Two-photon deep tissue ex vivo imaging of mouse dermal and subcutaneous structures," *Opt. Express* **3**(9), 339–350 (1998).
16. M. Ruggeri et al., "Retinal structure of birds of prey revealed by ultra-high resolution spectral-domain optical coherence tomography," *Investig. Ophthalmol. Visual Sci.* **51**(11), 5789–5795 (2010).
17. W. Song et al., "Integrating photoacoustic ophthalmoscopy with scanning laser ophthalmoscopy, optical coherence tomography, and fluorescein angiography for a multimodal retinal imaging platform," *J. Biomed. Opt.* (to be published).